# Experimental Determination of Conformational Isomerization Energy Thresholds in Serotonin

**Tracy A. LeGreve, Jasper R. Clarkson,† and Timothy S. Zwier***

*Department of Chemistry, Purdue University, West Lafayette, Indiana 47907-2084*

*Received: January 8, 2008; In Final Form: February 9, 2008*

Stimulated emission pumping-population transfer (SEP-PT) and hole-filling (SEP-HF) spectroscopies were used to determine the energy thresholds to isomerization between thirteen reactant−product conformer pairs in the biomolecule serotonin (SERO). Serotonin is a close structural analog of tryptamine (TRA), differing in having a hydroxyl group in the 5 position of the indole ring. A previous spectroscopic study (LeGreve; et al. *J. Am. Chem. Soc.* **2007**, *129* (13), 4028) identified eight conformational isomers of SERO, whose interconversion involves motion of the 3-ethylamine side chain, the 5-OH group, or both. In the cases in which only an ethylamine side chain reorientation occurred, the barriers were found to be similar to, but systematically somewhat smaller than, those in TRA, which has been studied by similar methods (Dian; et al. *Science* **2004**, *303* (5661), 1169; Clarkson; et al. *J. Chem. Phys.* **2005**, *122* (21), Art. No. 214311). In most cases, the experimental thresholds are well reproduced by calculated transition states separating the conformational wells; however, tunneling effects may artificially reduce the thresholds observed for isomerization of SERO(A,Gpy(out)) and SERO(B,Gpy(up)) into SERO(C,Gph(out)). The A → A′ isomerization involving only the OH rotation from *anti* to *syn* was found to be 721−761 $cm^{-1}$, in accordance with the calculated classical barrier. For isomerizations in which the ethylamine side chain reorients as does the OH group, the barriers to isomerization were consistent with sequential rather than concerted motion of both groups. Finally, some evidence for mode-specific effects in the product quantum yields near threshold is presented.

## I. Introduction

Serotonin (5-hydroxytryptamine, SERO) is a neurotransmitter that plays an important and versatile role in human physiology.[1−5] Its simple molecular structure (Figure 1, inset) makes it an ideal target for fundamental studies of its conformational preferences and isomerization dynamics. By studying the isolated molecule, one hopes to characterize the potential energy surface on which isomerization occurs in some detail, both for testing theoretical predictions and as benchmark studies for understanding the solvent's contributions to barriers and isomerization pathways.

Our previous study of the conformation-specific ultraviolet and infrared spectroscopy of SERO showed that, although there are at least eighteen possible conformational isomers, eight are seen in the jet expansion.[6] Figure 1 shows an LIF spectrum in the $S_1 \leftarrow S_0$ origin region of SERO, with labels indicating the conformations responsible for the transitions, based on our previous work. These eight conformers split into two groups depending on the orientation of the 5-hydroxy group, either *anti* ($\theta_1 = 180°$) or *syn* ($\theta_1 = 0°$) relative to indole NH. The five *anti*-OH origins are seen to the blue (higher wavenumber) of the three *syn*-OH origins.

The conformers observed in serotonin have close analogs in tryptamine (TRA), sharing the same preference for out-of-plane orientations of the ethylamine side chain ($\chi_1 \sim 90°$). These differ primarily in the position and orientation of the amino group, involving changes principally in two dihedral angles, $\chi_2$ and $\chi_3$. The amino group can reside in any one of three positions, *gauche* on the pyrrole side of indole (Gpy), *gauche* on the phenyl side (Gph), and *Anti*. The orientation of the amino group is labeled by the direction of the lone pair of electrons relative to the indole plane, indicated in parentheses.[6−8] Figure 2 shows a two-dimensional plot of the potential energy surface along

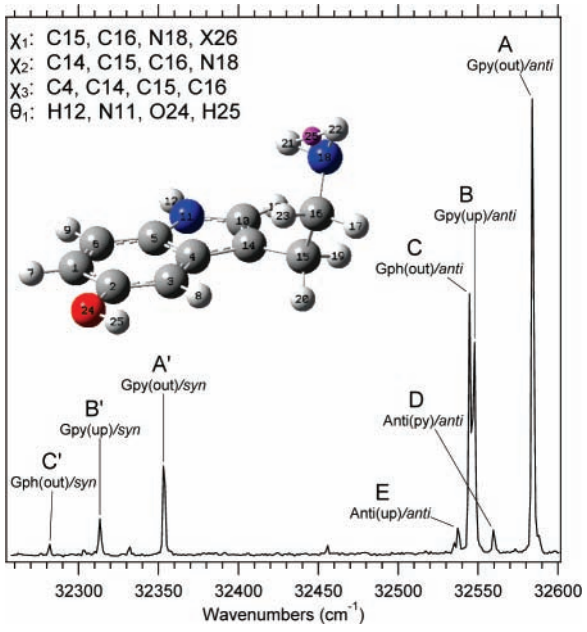


**Figure 1.** LIF scan of the $S_1 \leftarrow S_0$ origin region of SERO. Inset: 3-D structure of SERO (A) with the four dihedral angles defined.

* To whom correspondence should be addressed. E-mail: zwier@purdue.edu.

† Current address: Eastman Chemical Co., Tennessee Operations, P.O. Box 431, Kingsport, TN, 37662. E-mail: jclarkson@eastman.com.

10.1021/jp800165q CCC: $40.75 
Published on Web 03/27/2008

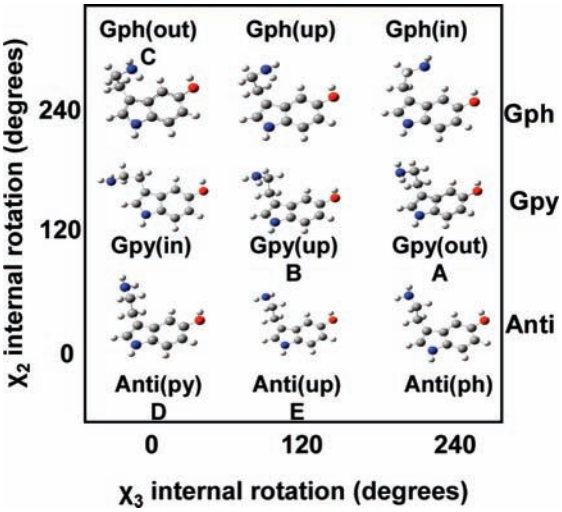


**Figure 2.** Schematic two-dimensional potential energy surface showing nine low-lying conformational minima of SERO *anti* OH.

the $\chi_2$ and $\chi_3$ dihedral angles for all nine possible conformations of the *anti* OH SERO molecule.

Firm assignments for the eight observed conformers of SERO were made on the basis of a comparison of the single-conformation infrared spectra of SERO and TRA in the alkyl CH stretch region, which are diagnostic of the ethylamine side chain conformation.[6] Not surprisingly, the conformational preferences in SERO are generally similar to those in TRA, with the most intense transitions in both molecules ascribable to the Gpy(out) ethylamine side chain conformation, labeled "A" in the figure. The Gph(out) conformation (C and C′) was enhanced in SERO relative to TRA, indicating that the 5-OH group plays an active role in modulating the relative energies of the conformations of the ethylamine side chain.

The present work builds on the previous spectroscopic study by measuring the energy thresholds to isomerization in isolated SERO. This work uses the method of stimulated emission pumping-population transfer (SEP-PT) and SEP hole-filling (SEP-HF) methods, which have been described in some detail previously.[8−11] These methods use a unique experimental protocol by which a single "reactant" conformation X is excited via SEP to a vibrational level in the ground electronic state with well-defined energy, thereby initiating conformational isomerization to any conformations for which the barrier to isomerization is below that energy. Following re-cooling in the supersonic expansion, a specific product conformation Y can be probed downstream. By tuning the energy imparted to the conformer in the SEP step, one can observe the threshold for isomerization from X to Y.

Once again, the natural point of comparison for the present work is with our previous SEP-PT study of the isomerization thresholds in TRA.[8,10] In comparison, SERO is rich in possibilities because it has a second flexible side chain (the 5-OH group). As a result, reactant−product pairs are probed that involve isomerization within the ethylamine side chain, within the OH group, or both. The results of our experimental study will be compared with the experimental thresholds in TRA and calculated barriers in SERO. In many cases, there is a good correspondence in both regards. As in TRA,[8,10] where differences do appear, there is the possibility that tunneling of the $NH_2$ group lowers the experimental thresholds below the corresponding classical barrier heights.

Finally, conformational isomerization in SERO is interesting in part because the two flexible side chains (the 5-OH group and the 3-ethylamine group) are quite different in size and are remote from one another. At a given internal energy, the vibrational density of states will be dominated by the many low-frequency torsional modes associated with the ethylamine side chain. In comparison, *syn* ↔ *anti* OH isomerization involves a single OH internal rotational coordinate, with a sparse vibrational structure. Initiating isomerization out of different types of vibrational levels could in principle lead to interesting, state-specific dynamics. As we shall see, our results touch on this possibility.

## II. Methods

**A. Calculations.** Minimum energy structures for the eight observed conformations of serotonin have been calculated previously at a range of levels of theory.[6,12] Here, these results are complemented by calculations of the transition states (TS) separating the observed minima for comparison with the experimentally measured energy thresholds for isomerization. The transition states were calculated with Gaussian03[13] using density functional theory (DFT) with the Becke3LYP[14,15] functional and the 6-31+G* basis set.[16] The QST3[17] algorithm was used for optimization. The transition states were confirmed as first-order transition states by the presence of a single vibration with imaginary frequency. Starting structures for the transition states that involve a rearrangement only of the ethylamine side chain were made on the basis of the dihedral angles of transition states previously calculated for tryptamine.[8]

**B. Experimental Details.** The chamber utilized for laser-induced fluorescence (LIF) and the experimental details of stimulated emission pumping (SEP), population transfer (SEP-PT) and hole-filling (SEP-HF) spectroscopies have been described previously.[8−10] Serotonin (SERO) was obtained commercially (Waco) and used without further purification. The sample was entrained by using helium as a carrier gas at a pressure of 7 bar. The sample was heated to 170 °C and pulsed into the vacuum chamber using a high-temperature pulsed nozzle (General Valve, Series 9, 1.2 mm diameter ($D$)) at 20 Hz. The LIF and SEP spectroscopies were carried out at 6.25 mm ($x$) from the nozzle orifice, which results in an $x/D = 5$.

The doubled output from three independent dye lasers each pumped by a separate Nd:YAG laser were used in this experiment. The first UV laser (20 Hz, R640 dye, 0.1−0.5 mJ) was used as a "pump" laser to excite a particular $S_1 \leftarrow S_0$ transition of interest. The second UV laser (10 Hz, DCM dye 0.5−1.0 mJ) was used as a "dump" laser to stimulate the emission from the excited state origin back down into specific vibrational levels in the ground state. These two lasers were utilized to acquire stimulated emission pumping (SEP) spectra from different conformational isomers of SERO using their respective $S_1 \leftarrow S_0$ origin transitions as pump transitions. The two lasers were spatially overlapped and separated in time by 2 ns, a delay chosen to maximize the SEP depletion signal. The SEP data are acquired by setting the pump laser (20 Hz) to a specific $S_1 \leftarrow S_0$ transition of interest while scanning the dump laser at 10 Hz to drive the excited state population back to specific vibrational levels in the ground state ($S_0(v)$). Under optimal conditions 25−35% of the population in the $S_1$ excited state of a specific conformation was driven back down to $S_0$-($v$).

The SEP data were recorded using an active baseline subtraction program where the signal is taken from a gated integrator and recorded with and without the 10 Hz dump laser present. This program is used to better monitor the total fluorescence signal and allows for better quantification of

**TABLE 1: Relative Energies (kcal/mol) and Wavenumbers (in Parentheses) of the Transition States of Serotonin Calculated Using B3LYP/6-31+G* with the QST3 Algorithm for Optimization**

| | *anti* | | *syn* | |
|---|---|---|---|---|
| transition state | from lower− energy minima | from higher− energy minima | from lower− energy minima | from higher− energy minima |
| Gpy(out)/Gpy(up) | 2.65 (929) | 2.49 (871) | 2.63 (922) | 2.43 (851) |
| Gpy(out)/Gpy(in) | 1.96 (685) | 0.79 (275) | 1.90 (665) | 0.79 (278) |
| Gpy(out)/Gph(in) | 6.19 (2167) | 4.12 (1441) | 6.04 (2113) | 3.42 (1196) |
| Gpy(out)/Anti(ph) | 3.88 (1359) | 3.43 (1200) | 3.92 (1372) | 3.31 (1157) |
| Gpy(up)/Gpy(in) | 4.39 (1536) | 3.38 (1184) | 4.32 (1513) | 3.42 (1197) |
| Gpy(up)/Gph(up) | 3.15 (1101) | 2.44 (855) | 3.10 (1086) | 2.54 (891) |
| Gpy(up)/Anti(up) | 3.72 (1302) | 3.45 (1208) | 3.72 (1301) | 3.52 (1233) |
| Gph(out)/Gph(up) | 3.45 (1207) | 2.79 (975) | 2.93 (1024) | 2.91 (1020) |
| Gph(out)/Gph(in) | 3.01 (1053) | 1.14 (399) | 2.34 (818) | 0.49 (172) |
| Gph(out)/Gpy(in) | 5.92 (2072) | 4.95 (1734) | 5.61 (1963) | 5.28 (1847) |
| Gph(out)/Anti(py) | 3.91 (1369) | 3.50 (1226) | 3.41 (1195) | 3.17 (1108) |
| Anti(py)/Gpy(in) | 3.26 (1142) | 2.71 (947) | 3.31 (1158) | 2.73 (956) |
| Anti(ph)/Anti(py) | 2.09 (731) | 1.93 (675) | 2.23 (780) | 2.14 (750) |
| Anti(up)/Anti(py) | 2.20 (770) | 2.02 (706) | 2.13 (747) | 2.00 (701) |
| Anti(up)/Gph(up) | 3.66 (1282) | 3.22 (1129) | 3.48 (1218) | 3.12 (1090) |
| Anti(up)/Anti(ph) | 2.11 (738) | 2.09 (730) | 2.36 (826) | 2.14 (750) |
| Gph(up)/Gph(in) | 3.23 (1129) | 2.02 (706) | 3.12 (1090) | 1.26 (439) |
| Gph(in)/Anti(ph) | 2.47 (865) | 0.85 (297) | 2.95 (1034) | 0.95 (331) |

depletion percentage. Each time the dump laser passes through a vibrational level in the ground state a depletion of fluorescence signal is seen.

Single-conformation dispersed fluorescence (DF) scans were recorded to compare with the SEP scans. The comparison is valid because both SEP and DF access ground state vibrational levels of a single conformation based on the same Franck−Condon factors. Both SEP and DF excite a single conformation but in SEP, the population is driven back into the ground state by tuning the dump laser, where in DF the resulting fluorescence from the excitation of the single conformation is brought into a monochromator where it gets dispersed with a resulting ground state vibrational spectrum. The experimental details for DF are described elsewhere.[18]

The three laser SEP-PT method has been described in detail previously.[8,10,11,19−21] In SEP-PT, the SEP step is carried out at $x/D = 2$ with the probe at $x/D = 5$. This results in a time separation of 1.8−2.0 $\mu$s between SEP and probe steps. The position of SEP excitation provides sufficient vibrational cooling to bring the populations of the conformers to their vibrational zero-point levels prior to the SEP step, but in a collisional region of the expansion where sufficient collisions occur between SEP and probe that the molecules excited by SEP can be re-cooled to the zero-point level prior to interrogation with the probe laser.

There are two different ways of executing the three-laser experiment: SEP-population transfer (PT) and hole-filling (HF). For SEP-PT, the pump and probe lasers (both at 20 Hz) were fixed on the $S_1 \leftarrow S_0$ origin transitions of reactant X and product Y, while the wavelength of the 10 Hz dump laser was scanned. This allowed the observation of population funneling from the conformer excited by the pump-dump laser combination into the conformer probed by the probe laser as a function of the internal energy in the excited conformer from the dump laser.

In SEP-HF, the wavelengths of the pump (20 Hz) and dump (10 Hz) lasers are fixed and the probe laser (20 Hz) is tuned. In this way, the products formed at a given dump internal energy appear as gain signals as the probe laser is tuned through the $S_1 \leftarrow S_0$ origin transitions of the various product conformations.

As was done in previous studies, two two-laser checks were utilized to optimize the population transfer and hole-filling signals. The first check was to maximize the 20 Hz dip between the pump and probe lasers when the wavelength of both lasers was fixed on the same transition due to a particular conformer. This was done downstream at $x/D = 5$. Second, once this dip was maximized, the pump laser was moved upstream to $x/D = 2$, with the timing of the pump laser adjusted to 1.8−2.0 $\mu$s earlier in time to maintain the 20 Hz dip. Then the dump laser was overlapped on top of the pump laser and SEP dip was maximized.

**TABLE 2: Relative Energies (kcal/mol) and Wavenumbers (in Parentheses) of the Transition of *anti* to *syn* OH Conformers of Serotonin Calculated Using B3LYP/6-31+G* with the QST3 Algorithm for Optimization**

| | from lower− energy minima | | from higher− energy minima | |
|---|---|---|---|---|
| transition state | TS1[a] | TS2[b] | TS1[a] | TS2[b] |
| Gpy(out) | 2.22 (778) | 2.30 (805) | 2.00 (700) | 2.08 (727) |
| Gpy(up) | 2.32 (812) | 2.26 (789) | 2.06 (720) | 1.99 (698) |
| Gph(out) | 2.63 (921) | 2.68 (937) | 1.84 (644) | 1.89 (660) |
| Anti(py) | 2.14 (749) | 2.20 (769) | 2.00 (701) | 2.06 (721) |
| Anti(up) | 2.23 (781) | 2.14 (750) | 2.04 (715) | 1.95 (684) |
| Gpy(in) | 2.17 (761) | 2.17 (760) | 2.01 (705) | 2.01 (705) |
| Gph(up) | 2.14 (750) | 2.21 (774) | 2.03 (709) | 2.09 (733) |
| Gph(in) | 2.65 (929) | 2.52 (883) | 1.89 (660) | 1.75 (614) |
| Anti(ph) | 2.28 (797) | 2.37 (831) | 1.89 (663) | 1.99 (697) |

[a] TS1: $\theta_1 = +90°$; possible interaction between the OH and ethylamine side chain. [b] TS2: $\theta_1 = -90°$; no interaction between the OH and ethylamine side is possible.

## III. Results and Analysis

**A. Calculations.** Table 1 summarizes the results of the transition state (TS) calculations for *anti* and *syn* OH serotonin involving rearrangement of the ethylamine side chain. In each case, the energies of the transition states were compared to the two minima connected by the transition state. Table 2 lists the calculated relative energies of the transition states that involve only an OH rotation. These TS energies are all very similar, as one might expect if the OH and ethylamine side chains are largely independent of one another. Note that there are two ways in which the OH can rotate, one in which the OH hydrogen swings to the same side as the ethylamine side chain, the other when it is on the opposite side. TS1 represents a $\theta_1 = +90°$ rotation and TS2 represents a $\theta_1 = -90°$ rotation relative to the side of the indole ring over which the ethylamine side chain is positioned, so a +90° rotation could possibly result in an

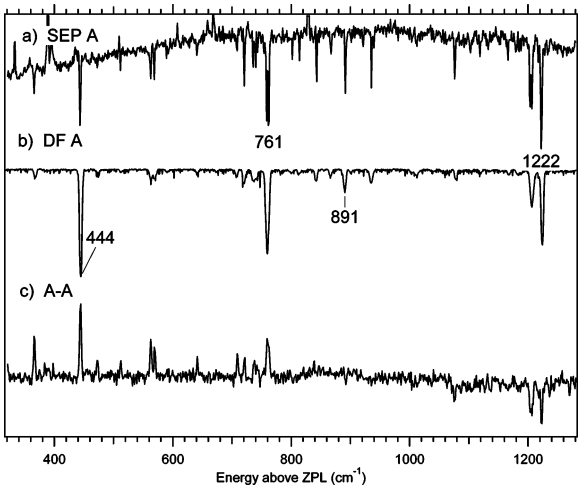


**Figure 3.** (a) SEP of SERO(A). (b) DF of SERO(A). (c) SEP-PT spectrum for the A → A reactant channel.

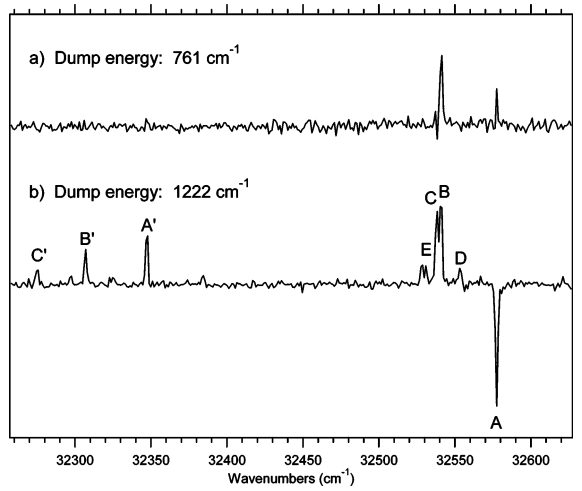


**Figure 4.** SEP-HF spectra of SERO(A) at dump energies that place (a) 761 $cm^{-1}$ and (b) 1222 $cm^{-1}$ of internal energy into SERO(A).

interaction between the OH and ethylamine side chain whereas a −90° rotation will have no possible interaction.

**B. Experimental Details.** Figure 3a presents the SEP spectrum of conformer A of serotonin. The horizontal axis is the difference in wavenumber between the pump and dump lasers and is labeled here and in subsequent figures as the internal energy given to the excited conformer (SERO(A) in this case) by the combination of pump and dump lasers. The SEP spectrum shows sharp dips in the fluorescence signal when the dump laser is resonant with a vibronic transition in SERO-(A), due to removal of a portion of the excited state population via stimulated emission. The DF spectrum of the $S_1$ origin of SERO(A) is shown in Figure 3b for comparison. It is clear from this comparison that the SEP spectrum relies on the same Franck−Condon factors that determine the intensities in spontaneous emission. Not surprisingly, the SEP spectrum enhances the intensities of small vibronic transitions due to saturation effects. The sharp gains in the SEP spectrum arise from interference from SERO-$H_2O$ transitions induced by the dump laser in this wavelength region. SEP, DF, and SEP-PT spectra for conformers B and C (Figure SM1) can be found in the Supporting Information.

Figure 4 compares SEP-HF spectra of SERO(A) recorded with the dump laser wavelength fixed on dump transitions back to $S_0$ vibrational levels in A that are 761 (Figure 4a) or 1222 $cm^{-1}$ (Figure 4b) above the zero-point level of A, labeled in Figure 3a. In both cases, the pump laser was fixed on the SERO-(A) $S_1 \leftarrow S_0$ origin transition. The spectrum in Figure 4b shows a strong depletion in the population of the "reactant" SERO-(A), and sizable gains in the populations of all seven other SERO conformers (B−E, A′−C′). This proves unequivocally that an internal energy of 1222 $cm^{-1}$ in SERO(A) is sufficient energy to overcome all barriers to isomerization to the other observed conformers of SERO. Furthermore, no gains are observed at other wavelengths, indicating that no new conformers are formed by the SEP/re-cooling process beyond those that are formed by cooling the thermal population present prior to supersonic expansion.

In contrast, the spectrum in Figure 4a has a small gain in the reactant SERO(A) signal, and in product conformers B, A′, and possibly B′. We surmise on this basis that 761 $cm^{-1}$ is above the barriers to these conformers but below those of the others. Furthermore, as will be explained in more detail in the following paragraph, the small *gain* in the "reactant" A population is some indication that isomerization is still rather inefficient at this energy, suggesting near-threshold behavior in which a fraction of the A population is re-cooled into the reactant well on a time scale that can compete with isomerization.

These deductions based on SEP-HF scans are strengthened by considering the A → A SEP-PT spectrum shown in Figure 3c. This scan was recorded by fixing the wavelength of both the pump and probe lasers on the $S_1 \leftarrow S_0$ origin of conformer A while scanning the dump laser wavelength. At low internal energy ($E$ < 761 $cm^{-1}$), strong gain signals are seen in the reactant channel A due to the dump laser returning population into the well of conformer A below all barriers to conformational isomerization. The A → A SEP-PT spectrum shows a gain signal for vibronic transitions below barriers to isomerization because the 20−10−20 Hz laser configuration highlights the difference in population induced by the dump laser. When the dump laser is off, the 20 Hz pump laser removes population from the SERO(A) $S_0$ zero-point level, much of which does not return to the ground state (e.g., via internal conversion or intersystem crossing), even under collisional cooling conditions. When the dump laser is on, however, a fraction of the excited population is returned to low-lying vibrational levels in the ground state of A, where they can be re-cooled into the zero-point level of A, effectively producing a gain in population whenever the dump laser is present.

A comparison of the SEP (Figure 3a) and SEP-PT (Figure 3c) scans shows a significant decrease in the relative size of the gain signal for the strong transition at 761 $cm^{-1}$, precisely where the SEP-HF spectrum showed near-threshold isomerization to SERO(B) and SERO(A′). Furthermore, higher-lying vibronic transitions are first reduced in intensity, and then become depletions rather than gains, as is clearly evident for the strong vibronic transitions near 1200 $cm^{-1}$. The qualitative deduction that can be drawn from this crossover from gain to depletion is that in the higher-energy region, the dump laser is accessing vibrational levels of SERO(A) where isomerization occurs to a greater and greater extent, thereby siphoning off a larger and larger fraction of the population into other conformational wells.

In earlier work on *meta*-divinylbenzene,[11] we presented a detailed analysis of the signal intensities in SEP-PT spectroscopy. The conclusion drawn from these studies, and confirmed here, is that these depletions in the reactant channel arise from the synergistic effect of pump and dump lasers, which are partially overlapped in time, removing a greater fraction of the ground state population of A when both pump and dump are

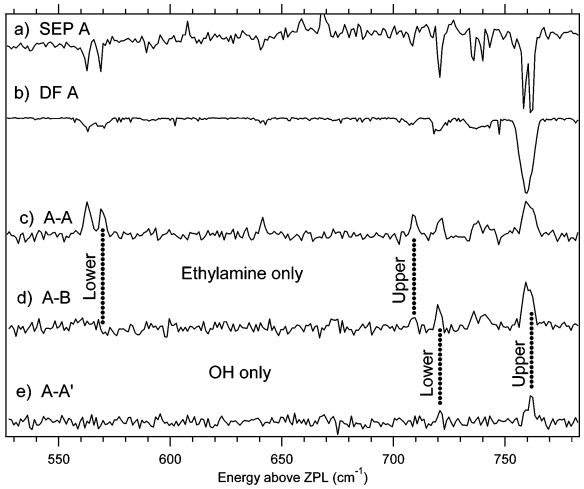


**Figure 5.** (a) SEP of SERO(A). (b) DF of SERO(A). SEP-PT spectrum of SERO (c) A → A, (d) A → B, and (e) A → A′, over the 530−780 $cm^{-1}$ energy range.

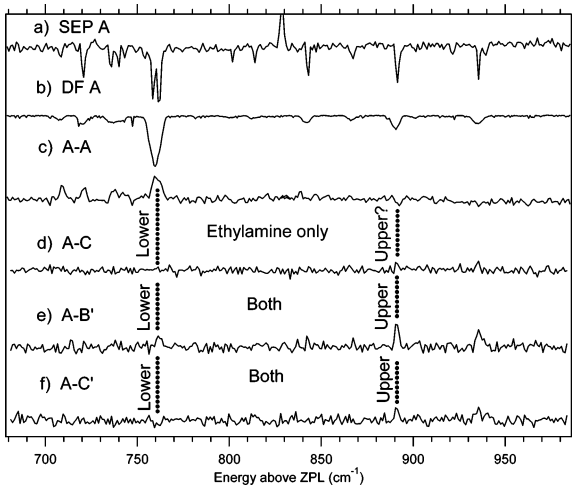


**Figure 6.** (a) SEP of SERO(A). (b) DF of SERO(A). SEP-PT spectrum of serotonin (c) A → A, (d) A → C, (e) A → B′, and (f) A → C′ in the 680−980 $cm^{-1}$ energy range.

resonant with strong vibronic transitions well above the barriers to isomerization. Under these conditions, fast isomerization from the vibrational levels accessed by the dump laser can mitigate the effects of saturation in the dump step, thereby enabling a greater transfer of population from the $S_0$ zero-point level of A to $S_0(v)$ and on to products.

On the basis of the results of Figures 3 and 4, it is clear that dump wavelengths spanning the internal energy range 500−1300 $cm^{-1}$ will be required to determine the energy thresholds for isomerization out of SERO(A). To establish thresholds most clearly, Figures 5−7 present close-up views of three overlapping regions in this range. In each case, we present only those A → X product channels that show some evidence of a gain signal that indicates an energy threshold to that channel has been overcome. In a couple of cases, this threshold is uncertain given the signal-to-noise ratio available in the SEP-PT spectrum, and in those cases, separate SEP-HF scans fixed on the dump transition(s) of interest will be considered to establish the threshold more firmly.

The 520−780 $cm^{-1}$ region of the SEP-PT spectra for A → A, A → B, and A → A′ are shown in Figure 5c−e, respectively, and the SEP and DF spectra of SERO(A) are shown above them in Figure 5a,b for comparison in locating the thresholds of interest. The first "gain" peak observed in a particular A → X

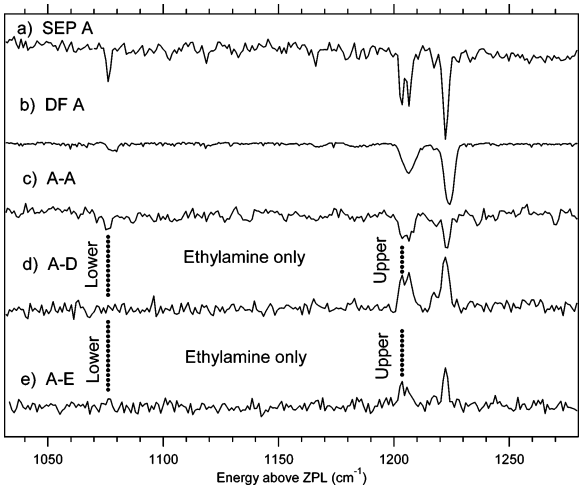


**Figure 7.** (a) SEP of SERO(A). (b) DF of SERO(A). SEP-PT spectra of serotonin (c) A → A, (d) A → D, and (e) A → E in the 1030−1275 $cm^{-1}$ energy range.

**TABLE 3: Comparison of Experimentally Determined Energy Isomerization Barriers for Serotonin and Tryptamine (in Energy above ZPL)**

| reactant → product | serotonin ($cm^{-1}$ above ZPL) | tryptamine[a] ($cm^{-1}$ above ZPL) |
|---|---|---|
| Gpy(out) → Gpy(up) | 569−710 | 688−748 |
| Gpy(out) → Gph(out) | 761−843 | 860−1000 |
| Gpy(out) → Anti(py) | 1076−1204 | 1219−1316 |
| Gpy(out) → Anti(up) | 1076−1204 | 1219−1316 |
| Gpy(up) → Gpy(out) | 444−759 | <562 |
| Gpy(up) → Gph(out) | 444−759 | <747 |
| Gph(out) → Gpy(out) | 758−1225 | |
| Gph(out) → Gpy(up) | 758−1225 | <747 |
| Gpy(out)/*anti* → Gpy(out)/*syn* | 721−761 | |
| Gpy(out)/*anti* → Gpy(up)/*syn* | 761−891 | |
| Gpy(out)/*anti* → Gph(out)/*syn* | 761−891 | |
| Gpy(up)/*anti* → Gpy(out)/*syn* | 444−759 | |
| Gph(out)/*anti* → Gpy(out)/*syn* | 758−1225 | |

[a] Experimental data from Clarkson et al.[8] and Dian et al.[10]

SEP-PT spectrum that lines up with a peak from the SEP of the reactant A is thereby established as an upper bound to the energy barrier to isomerization from A to X. The wavenumber position of an SEP transition lower in energy that is not observed constitutes a lower bound to the barrier, barring a significant kinetic shift. The upper and lower bounds so determined are marked by dotted lines on the A→ B and A → A′ SEP-PT scans. In the A → B spectrum, all the transitions in the closely spaced group between 700 and 770 $cm^{-1}$ are observed, but gain signals associated with transitions at 640, 569, and 563 $cm^{-1}$ are not detected. Because the transition at 640 $cm^{-1}$ is so weak, we were not able to firmly establish it as a lower bound, and Table 3 includes the conservative value of 569 $cm^{-1}$ instead.

A comparison of the relative intensities of the SEP (Figure 5a) and A → B SEP-PT transitions (Figure 5d) in the 700−770 $cm^{-1}$ region show a reduced intensity in SEP-PT for the band at 721 $cm^{-1}$, with other bands above this reflecting their intensity in SEP. This provides another indication that the 721 $cm^{-1}$ transition is just above the energy threshold for isomerization, where collisional cooling to below threshold can compete with isomerization.

A firm upper bound for the A → A′ isomerization is established by the gain signal observed at 761 $cm^{-1}$. None of the other transitions below this energy are clearly evident, despite the fact that the corresponding transitions in the A → B and A → A spectra are clearly seen with intensities that would

indicate that they should also be seen in A → A′ if energetically possible. As a result, we place a lower bound at 721 $cm^{-1}$ for A → A′, the strongest of the transitions not observed in this region.

The structural changes associated with the A → B and A → A′ thresholds are nicely complementary to one another. The A → B isomerization involves a reorientation of the $NH_2$ group in the ethylamine side chain from Gpy(out) to Gpy(up), with no change in the OH group, and A → A′ involves a hindered rotation of the 5-OH group on the indole ring, with no change in the ethylamine side chain. That the two thresholds are in close proximity to one another is most likely nothing more than an interesting coincidence.

Figure 6d−f displays the SEP-PT spectra of A → C, A → B′, and A → C′ in the 680−980 $cm^{-1}$ region, respectively. These are juxtaposed, as before, with the SEP (Figure 6a), DF (6b), and A → A reactant SEP-PT spectra (6c) for comparison. The A → C isomerization involves a reorientation of the ethylamine side chain from Gpy(out) to Gph(out), retaining the *anti* OH configuration. In contrast, the A → B′ (Gpy(out)/*anti* → Gpy-(up)/*syn*) and A → C′ (Gpy(out)/*anti* → Gph(out)/*syn*) events involve both a reorientation of the ethylamine side chain and a 180° internal rotation of the 5-OH group in the indole ring from *anti* to *syn*.

Clear upper bounds to the energy thresholds are observed at 891 $cm^{-1}$ for the A → B′ and A → C′ isomerizations (Figure 6e,f), whereas the transitions at 843 and 761 $cm^{-1}$ are missing in both spectra. The intense transition at 761 $cm^{-1}$ in the SEP spectrum provides a firm lower bound to both thresholds, and the weaker transition at 843 $cm^{-1}$ should also have been observable, but with an intensity near the limit of our signal-to-noise ratio. As a result, Table 3 lists 761 $cm^{-1}$ as a firm lower bound and 843 $cm^{-1}$ as a probable lower bound.

When the A → C isomerization pair was probed in SEP-PT (Figure 6d), a very weak gain signal could be observed for the transition at 936 $cm^{-1}$ and perhaps hints of a signal at 891 $cm^{-1}$, but the signal is so weak that it was not possible to place bounds on the thresholds to isomerization on this basis. As a result, SEP-HF scans will be used to do so.

Parts d and e of Figure 7 show the SEP-PT spectra for A → D and A → E, where they are compared to the SEP (Figure 7a), DF (Figure 7b) and A → A reactant SEP-PT (Figure 7c) spectra of SERO(A). The lower and upper bounds for both the A → D and A → E isomerization were found to be 1076−1204 $cm^{-1}$. Unfortunately, the lack of strong SEP transitions between these two bounds keeps us from placing narrower limits on the threshold to isomerization in these cases. Both of these isomerizations involve an ethylamine reorientation from Gpy-(out) to Anti(py) for A → D and Gpy(out) to Anti(up) for A → E. All seven product channels show strong gains at 1204 and 1222 $cm^{-1}$, consistent with the hole-filling scan with dump laser fixed at 1222 $cm^{-1}$ presented previously in Figure 4b.

To provide checks on these thresholds and to determine the threshold for A → C, SEP-HF scans (Figure 8a−e) were recorded with the dump laser fixed on SEP transitions at 761, 843, 891, 936, and 1222 $cm^{-1}$, respectively. The crossover from gain to depletion in the reactant channel "A" with increasing internal energy in SERO(A) is clearly evident in the SEP-HF scans. With the dump laser fixed on the SEP transition at 761 $cm^{-1}$, the product gain signal is almost entirely due to SERO-(B), accompanied by a barely discernible gain in the SERO-(A′) product signal. Although conformer C is not seen at 761 $cm^{-1}$ (Figure 8a), it is clearly observed in the SEP-HF spectrum at 843 $cm^{-1}$ (Figure 8b) and in all scans with the dump laser

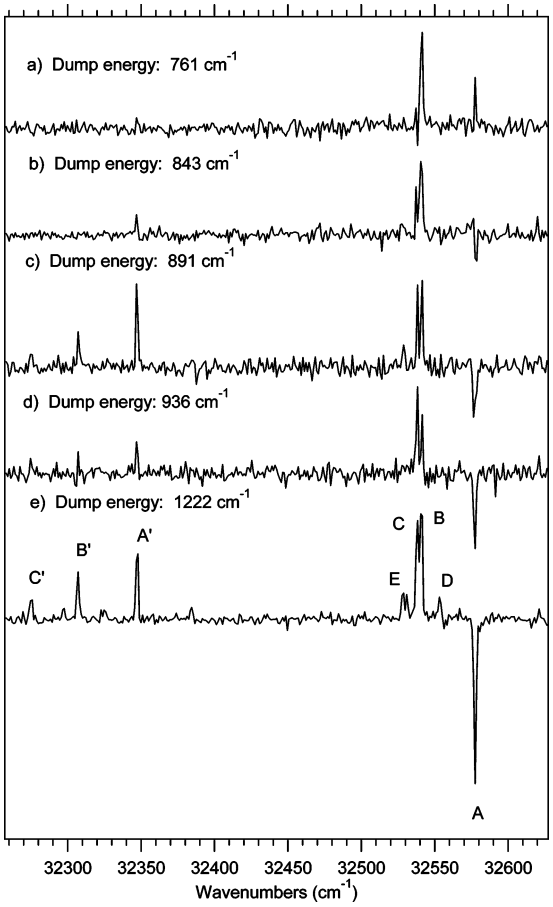


**Figure 8.** SEP-HF spectra with the dump laser fixed at (a) 761 $cm^{-1}$, (b) 843 $cm^{-1}$, (c) 891 $cm^{-1}$, (d) 936 $cm^{-1}$, and (e) 1222 $cm^{-1}$ above the zero-point level of SERO(A).

reaching levels with higher internal energy (Figure 8c-e). This places a firm upper bound for the A → C threshold at 843 $cm^{-1}$ (Table 3). Other thresholds observed in the SEP-HF spectra are consistent with those deduced from the SEP-PT spectra of Figures 5−7. The scan at 1222 $cm^{-1}$, reproduced from Figure 4b for comparison with the other scans, clearly shows the full slate of SERO conformer products. It is also worth noting that the intensities of the *syn* OH products (A′, B′, and C′) appear to be enhanced in the spectrum at 891 $cm^{-1}$ (Figure 8c) relative to their signals using dump transitions at higher and lower energy (Figure 8b,d).

SEP-HF spectra were also recorded following excitation of conformers B and C. Due to small signal levels, SEP-HF scans are only reported using the two intense SEP transitions at 759/758 $cm^{-1}$ (Figure 9b,c) and 1222/1225 $cm^{-1}$ (Figure 9d,e). Even then, only transitions involving the four largest population conformers (A, B, C, and A′) give measurable gain signals. The SEP-HF spectrum at the 759 $cm^{-1}$ transition of conformer B shows population transfer predominantly to A, with small gains at transitions due to C and A′. The corresponding scan for conformer C does not show any population gains, indicating that this energy is below all barriers to isomerization out of the conformer C well. At 1222/1225 $cm^{-1}$, excitation of both B and C produces the other three conformers, as expected.

## IV. Discussion

The measured energy thresholds to conformational isomerization in serotonin involve isomerization of the OH group (*syn* ↔ *anti*), the ethylamine side chain, or both. Table 3 summarizes

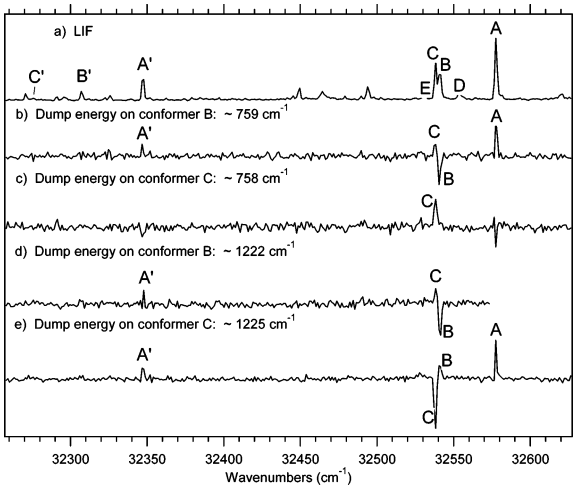


**Figure 9.** (a) LIF spectrum of SERO in the origin region. SEP-HF spectra taken with the dump laser fixed at b) 759 $cm^{-1}$, c) 758 $cm^{-1}$, d) 1222 $cm^{-1}$, and e) 1225 $cm^{-1}$ above the zero-point level of SERO-(B) and SERO(C), respectively.

the lower and upper bounds on the energy thresholds. As we have discussed in some detail previously,[8−11] in SEP-PT spectroscopy, the first dump transition in X where gain signal is observed in product channel Y provides an upper bound to the energy barrier to X → Y isomerization, except under conditions in which tunneling is present. The last unobserved transition is a lower bound to the barrier as long as the time scale for isomerization is fast compared to the rate of vibrational relaxation to energies below the barrier.

Because serotonin differs from tryptamine only in the addition of an OH group in the 5 position on the indole ring, it is useful to compare the observed thresholds with those measured previously in tryptamine. In cases where the isomerization involves only the ethylamine side chain (the top eight rows in Table 3), the comparison is very direct. Not surprisingly, the indicated ranges are quite similar, but slightly lower in serotonin. In several cases, the upper bound in serotonin is very close to the lower bound in tryptamine, indicating a small shift toward lower energy in the barriers to reorientation of the ethylamine side chain in serotonin.

Table 4 compares the calculated energies of the transition states involving the ethylamine side chain in serotonin (*anti* OH) and tryptamine. The calculated barriers out of conformer A (Gpy(out)) are lower than those in tryptamine by about 10−20%, consistent with the experimental trends just noted.

For most A → X reactant−product pairs, the observed lower and upper bounds are also in reasonable agreement with the calculated, zero-point corrected barriers to isomerization (Table 1). Figure 10 visualizes this comparison in terms of the two-dimensional potential energy surface involving $\chi_2$ and $\chi_3$, the primary ethylamine side chain coordinates involved in the ethylamine side chain isomerizations The green numbers are the experimentally determined energy barriers, and the maroon numbers are the calculated energy barriers all relative to SERO(A). In tryptamine, one notable exception to the close correspondence between experiment and theory was the A → F isomerization threshold, for which the experimental threshold was almost a factor of 2 lower in energy than the calculated classical barrier. This isomerization, which involves both a change of the position and orientation of the $NH_2$ group (Gpy-(out) → Gph(up)), was shifted by 90 $cm^{-1}$ to higher energy upon deuterium substitution on the amino group, indicating that tunneling was indeed playing a role in lowering the barrier relative to calculation.[8] In serotonin, conformer F is not observed; however, the A → C isomerization in serotonin (Gpy-(out) → Gph(out)) is somewhat analogous, and the calculated lowest-energy pathway from A to C involves the traversal (shaded in the figure) from A → B → F → C. The highest-energy barrier in this sequence is calculated to be 1279 $cm^{-1}$ above A, well above the experimental bounds for the process (761−843 $cm^{-1}$). Furthermore, the experimental upper bound on the B → C isomerization is 759 $cm^{-1}$, well below the calculated lowest-energy pathway, which involves traversal of barriers of 1158 and 1279 $cm^{-1}$. In the present case, we have not studied the deuterated isotopomers experimentally. However, it seems likely that the $NH_2$ group is involved in tunneling associated with the Gpy → Gph isomerization. Further theoretical exploration of this possibility would be helpful.

**TABLE 4: Comparison of Calculated Transition State Energies between *anti*-OH Serotonin and Tryptamine Calculated Using B3LYP/6-31+G* with the QST3 Algorithm for Optimization**

| | serotonin (*anti*-OH) | | tryptamine[a] | |
|---|---|---|---|---|
| transition state | from lower−energy minima | from higher−energy minima | from lower−energy minima | from higher−energy minima |
| Gpy(out)/Gpy(up) | 2.65 (929) | 2.49 (871) | 3.02 (1057) | 2.76 (966) |
| Gpy(out)/Gpy(in) | 1.96 (685) | 0.79 (275) | 2.42 (847) | 1.25 (438) |
| Gpy(out)/Gph(in) | 6.19 (2167) | 4.12 (1441) | 6.34 (2219) | 3.68 (1288) |
| Gpy(out)/Anti(ph) | 3.88 (1359) | 3.43 (1200) | 4.11 (1439) | 3.38 (1183) |
| Gpy(up)/Gpy(in) | 4.39 (1536) | 3.38 (1184) | 3.58 (1253) | 2.67 (935) |
| Gpy(up)/Gph(up) | 3.15 (1101) | 2.44 (855) | 4.43 (1551) | 3.85 (1348) |
| Gpy(up)/Anti(up) | 3.72 (1302) | 3.45 (1208) | 3.94 (1379) | 3.61 (1264) |
| Gph(out)/Gph(up) | 3.45 (1207) | 2.79 (975) | 3.33 (1166) | 3.03 (1061) |
| Gph(out)/Gph(in) | 3.01 (1053) | 1.14 (399) | 2.64 (924) | 0.51 (179) |
| Gph(out)/Gpy(in) | 5.92 (2072) | 4.95 (1734) | 6.10 (2135) | 5.46 (1911) |
| Gph(out)/Anti(py) | 3.91 (1369) | 3.50 (1226) | 3.73 (1306) | 3.53 (1236) |
| Anti(py)/Gpy(in) | 3.26 (1142) | 2.71 (947) | 3.33 (1166) | 2.89 (1012) |
| Anti(ph)/Anti(py) | 2.09 (731) | 1.93 (675) | 1.53 (536) | 1.53 (536) |
| Anti(up)/Anti(py) | 2.20 (770) | 2.02 (706) | 2.46 (861) | 2.31 (809) |
| Anti(up)/Gph(up) | 3.66 (1282) | 3.22 (1129) | 3.62 (1267) | 3.37 (1180) |
| Anti(up)/Anti(ph) | 2.11 (738) | 2.09 (730) | 2.54 (889) | 2.40 (840) |
| Gph(up)/Gph(in) | 3.23 (1129) | 2.02 (706) | 4.38 (1533) | 2.56 (896) |
| Gph(in)/Anti(ph) | 2.47 (865) | 0.85 (297) | 2.78 (973) | 0.86 (301) |

[a] Clarkson et al.[8]

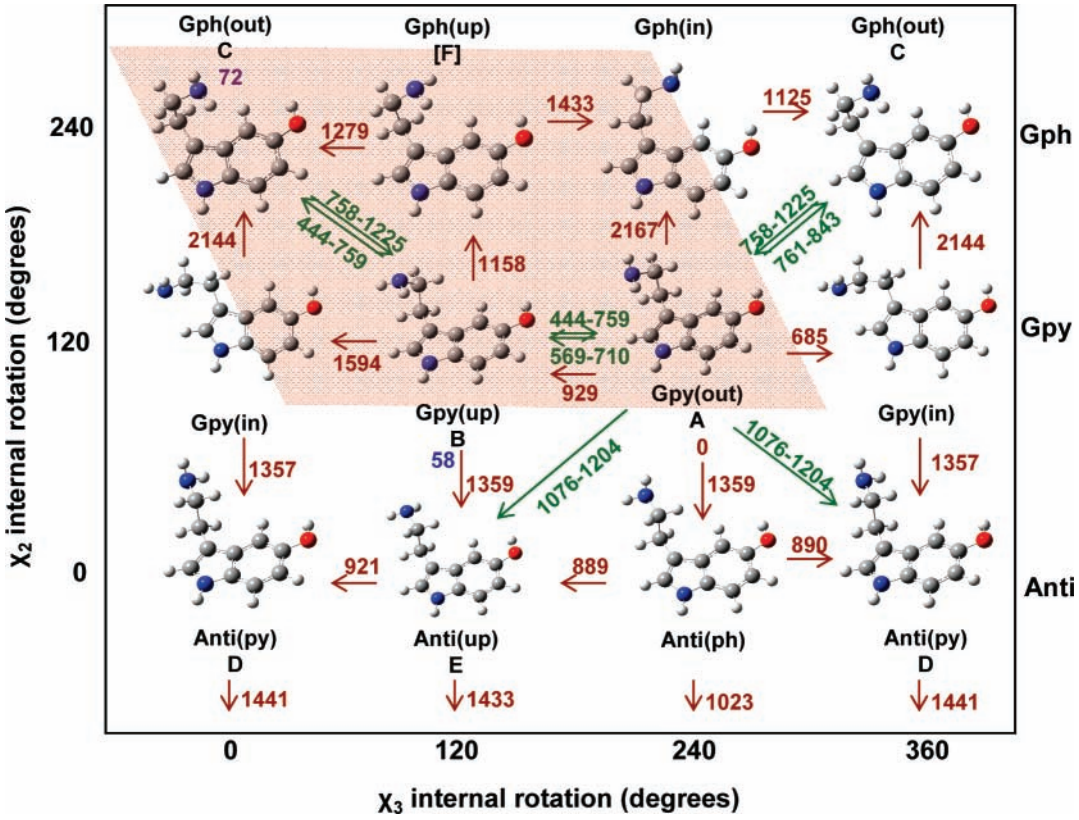


**Figure 10.** Two-dimensional potential energy surface for the low-energy *anti* OH conformers of SERO with the experimental (green) and calculated (maroon) energy barriers to isomerization in wavenumbers relative to SERO(A) = 0. The calculated relative energies for SERO(B) and SERO(C) minima are 58 and 72 $cm^{-1}$ above SERO(A), respectively. Gph(up) is labeled [F] because it is a conformer observed in tryptamine but not in serotonin.

The lower and upper bounds observed for isomerization of the OH group from *anti* to *syn* (A → A′) is 721−761 $cm^{-1}$, in close correspondence with the calculated, zero-point energy corrected barrier (778 or 805 $cm^{-1}$, with $\theta_1$ being +90° or −90°, respectively). Because this hindered rotation primarily involves motion of the OH hydrogen, tunneling could plausibly have lowered the threshold below its classical limit; however, this appears not to produce a significant lowering of the experimental threshold, assuming the correspondence not to be accidental.

From a dynamical standpoint, perhaps the most intriguing results are those involving isomerization of both the ethylamine and OH groups (e.g., A → B′ or A → C′). In those cases, the two-dimensional cut of the potential energy surface shown in Figure 10 for the *anti* OH isomers must be complemented by a second 2D surface associated with the *syn* OH group. The isomerization pathway then involves motion along at least three internal coordinates: $\chi_2$, $\chi_3$, and $\theta_1$ (the OH internal rotation coordinate). Consider, for instance, the A(Gpy(out)/*anti* OH) → C′(Gph(out)/*syn* OH) isomerization. The experimental lower and upper bounds placed on this isomerization are 761−891 $cm^{-1}$. At its simplest, the experimental result establishes that a sequential rather than concerted pathway is involved; that is, isomerization occurs in one flexible side chain at a time, rather than in both simultaneously, where the barrier height would be approximately the sum of the individual A → C and A → A′ isomerizations (∼1400 $cm^{-1}$).

Beyond this, it is not possible based on the present data to establish whether there is a single sequential isomerization pathway that dominates the others. In fact, we would anticipate that the two regions of the potential energy surface associated with OH and ethylamine side chains to be largely decoupled from one another, leading to several nearly isoenergetic sequential pathways (e.g., A → B → F → C → C′ or A → A′ → B′ → F′ → C′) with similar rate-limiting barriers. In such circumstances, it is likely that the whole collection of these pathways all contribute to the isomerization. The intramolecular vibrational energy redistribution that must accompany these different pathways involves states with a distribution of vibrational excitation in the OH and ethylamine side chains. Near threshold, those that promote isomerization from A → C′ are those with many quanta in the OH and none in the ethylamine side chain (e.g., for the A → A′ step) or vica versa (for the other steps). Classically, this corresponds to energy flow back and forth between the two independent side chains during the overall isomerization process.

In our earlier study of the single-conformation spectroscopy of serotonin,[6] we pointed out the increased intensity of transitions due to the Gph(out) conformer (SERO(C)) relative to the analogous transitions in TRA, consistent with a selective stabilization of this conformer in SERO. The present data provide further evidence for this fact. The observed upper bound for the A → C isomerization is 843 $cm^{-1}$, and the lower limit for the C → A threshold is 758 $cm^{-1}$. This establishes an upper bound for the energy difference between C and A of only 85 $cm^{-1}$:

$$E_C - E_A = E_{thresh}(A \rightarrow C) - E_{thresh}(C \rightarrow A) = (<843) - (>758) < 85\ cm^{-1}$$

The source of this selective stabilization of conformer C has not been firmly established[6] but is consistent with the alignment of the OH and $NH_2$ dipoles in Gph(out)/*anti* OH.

Finally, the SEP-HF spectra of Figures 8 and 9 provide an opportunity to comment on the conformational product distribu-

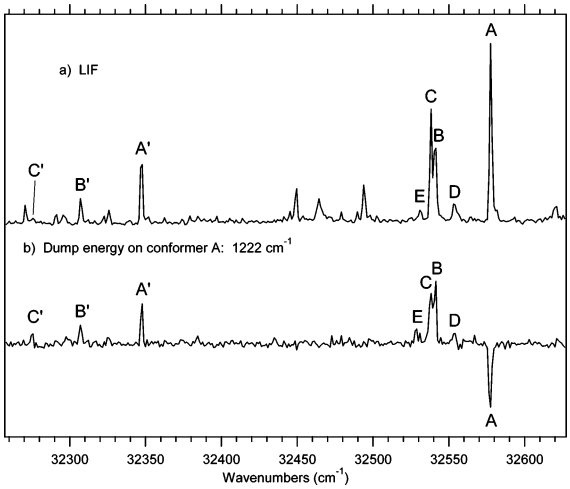


**Figure 11.** (a) LIF spectrum of SERO in the $S_0 \leftarrow S_1$ origin region. The transitions not labeled are due to the SERO-$H_2O$ complex. (b) SEP-HF spectrum with the dump laser fixed on a transition 1222 $cm^{-1}$ above the zero-point level of SERO(A).

tions formed by single-conformation SEP. The most important function of these spectra was as a means to determine the energy thresholds for isomerization involving specific reactant−product isomer pairs. However, the relative intensities also showed the competition between the different energetically accessible products.

Figure 11 compares the SEP-HF spectrum out of SERO(A) at 1222 $cm^{-1}$ (Figure 11b) with the corresponding LIF scan taking under identical conditions in the expansion (Figure 11a). This energy is above all the barriers to isomerization. If isomerization is fast compared to vibrational relaxation, we anticipate that well above the barriers to isomerization, the relative conformer populations will reach quasi-equilibrium prior to collisional quenching of further isomerization. The fact that the SEP-HF spectrum shows intensities so similar to those in the LIF spectrum argues for establishment of this quasi-equilibrium at 1222 $cm^{-1}$ internal energy in our experiment.

On the other hand, the SEP-HF spectrum at 891 $cm^{-1}$ (Figure 8c) shows a much greater intensity in A′, B′, and C′ products than its higher-energy counterpart at 936 $cm^{-1}$ (Figure 8d). This result seems to indicate that the 891 $cm^{-1}$ level in SERO(A) is more efficient than the 936 $cm^{-1}$ level in initiating isomerization involving OH internal rotation. We cannot state unequivocally that this is a state-selective difference because the reported spectra are each an average of two scans, from which we cannot establish error bars on the measurement. Nevertheless, the intensity difference was reproducible between the two scans. The transition at 891 $cm^{-1}$ can be assigned with some confidence to $14_2^0$, given the strong $14_1^0$ fundamental at 444 $cm^{-1}$ in the DF spectrum of SERO(A) (Figure 3b). As shown in Figure 12a, this mode is an in-plane ring distortion with substantial motion of the 5-OH group, providing a plausible argument that its initial excitation could facilitate OH internal rotation over the 721−761 $cm^{-1}$ OH internal rotation barrier.

The corresponding assignment of the 936 $cm^{-1}$ transition is less clear. Table 5 lists the calculated vibrational frequencies for a selected set of vibrations of SERO(A) in the 800−1200 $cm^{-1}$ region in comparison to the modes calculated for tryptamine by Schmitt et al.[22] The best match with the 936 $cm^{-1}$ level is as the $31_1^0$ fundamental of SERO(A), with calculated frequency of 956 $cm^{-1}$. A similar vibration at 1037 $cm^{-1}$ in tryptamine is assigned by Schmitt et al.[22] to a $CH_2$ twist, with principal motion in the ethylamine side chain. If this vibration

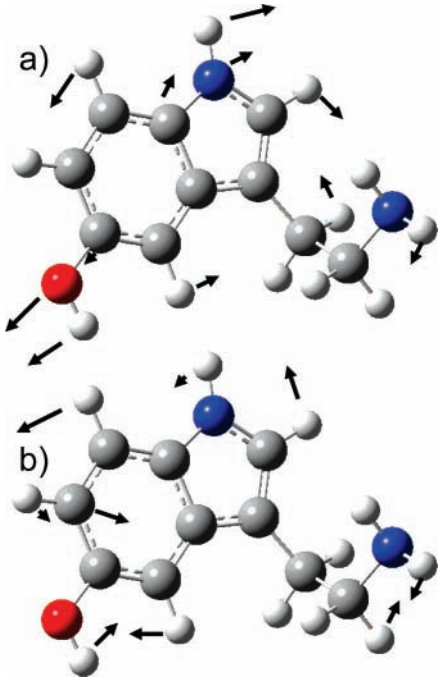


**Figure 12.** Normal mode vectors for the calculated vibrational modes (a) 14 and (b) 31 of SERO(A) with calculated frequencies of 455 and 956 $cm^{-1}$, respectively.

**TABLE 5: Comparison of the Calculated Ground State Vibrational Frequencies between TRA(A)[a] and SERO(A)**

| mode[a] | tryptamine[a] $S_0$ MP2/6-311G(d,p) | serotonin $S_0$ B3LYP/6-31+G* | exptl |
|---|---|---|---|
| 1 | 770 | 772 | 761 |
| $C_\alpha H_2$ twist | 878 | 860 | 843 |
| CCN bend | 469 × 2 = 938 | 455 × 2 = 910 | 891 |
| $CH_2$ twist/indole distortion | 1037 | 956 | 936 |
| OH bend[b] | | 1191 | |
| 13 | 1265 | 1255 | 1222 |

[a] Mode definitions and $S_0$ MP2 frequencies in tryptamine from Schmitt et al.[22] [b] OH bend specific to SERO.

were to truly be localized in the ethylamine side chain, where the low-frequency torsions would act as a repository for the vibrational energy, it could slow the rate of energy transfer to the remote 5-OH group. However, a close inspection of the tryptamine vibration indicates that it has significant indole ring motion as well. This carries over to the corresponding mode in SERO(A) (Figure 12b), which also involves significant stretching of the C−O bond. Based on these forms of the modes involved in SERO (Figure 12a,b), it is difficult to understand the seeming mode-specific differences in the experimental data.

It is possible that even subtle differences in the starting point in phase space could modulate the efficiency with which the OH internal rotation barrier is overcome near threshold. Because OH internal rotation involves a single vibrational coordinate, at a given energy, the density of states localized in the OH group is far less than in the ethylamine side chain. Once intramolecular vibrational energy redistribution (IVR) is complete, the ethylamine side chain would dominate the vibrational density of states, effectively soaking up energy in a portion of the molecule spatially removed from the 5-OH group, and thereby slowing the rate of isomerization over the OH internal rotation barrier. In the future, it will be interesting to explore isomerization in other molecules with remote side chains of varying size, where laser preparation can initially localize excitation in one or the other group.

## V. Conclusion

The techniques of SEP, SEP-PT, and SEP-HF spectroscopies were used to find the energy barriers to isomerization for the biologically important molecule serotonin. In cases where only the ethylamine side chain was involved, the measured thresholds were generally similar to those in tryptamine, a close analog of serotonin without the 5-OH group on the indole ring. In at least a couple of cases (A → C and B → C), the experimental thresholds were lower than the calculated transition states by an amount that suggests the possible contribution to isomerization from tunneling involving the $NH_2$ group. The barrier to hindered rotation of the OH group at the 5-position on the indole ring is 721−761 $cm^{-1}$, consistent with the calculated classical barrier. When internal energies in excess of 1200 $cm^{-1}$ are given to SERO(A), it produces a distribution of product populations similar to that produced by cooling the Boltzmann distribution present in the heated nozzle ($T_{nozzle} \sim 445$ K). However, near threshold for OH internal rotation, there is some evidence for state selectivity in the product yields. This suggests that other molecules with spatially separated flexible side chains be studied by the present experimental methods. Further theoretical modeling of the potential energy surface and isomerization dynamics of serotonin is also needed.

**Acknowledgment.** We gratefully acknowledge the National Science Foundation (Grant CHE-0551075) for support of this research. T.A.L. is grateful to the U.S. Department of Education for a Graduate Assistance in Areas of National Need Fellowship.

**Supporting Information Available:** The SEP, DF, and SEP-PT spectra of conformers B and C are presented in Figure SM1. This information is available free of charge via the Internet at http://pubs.acs.org.

## References and Notes

(1) Adayev, T.; Ranasinghe, B.; Banerjee, P. *Biosci. Rep.* **2005**, *25* (5−6), 363.
(2) Chaouloff, F.; Berton, O.; Mormede, P. *Neuropsychopharmacology* **1999**, *21* (2), S28.
(3) Hariri, A. R.; Holmes, A. *Trends Cognitive Sci.* **2006**, *10* (4), 182.
(4) Jouvet, M. *Neuropsychopharmacology* **1999**, *21* (2), S24.
(5) Pucadyil, T. J.; Kalipatnapu, S.; Chattopadhyay, A. *Cell. Mol. Neurobiol.* **2005**, *25* (3−4), 553.
(6) LeGreve, T. A.; Baquero, E. E.; Zwier, T. S. *J. Am. Chem. Soc.* **2007**, *129* (13), 4028.
(7) Carney, J. R.; Zwier, T. S. *J. Phys. Chem. A* **2000**, *104* (38), 8677.
(8) Clarkson, J. R.; Dian, B. C.; Moriggi, L.; DeFusco, A.; McCarthy, V.; Jordan, K. D.; Zwier, T. S. *J. Chem. Phys.* **2005**, *122* (21) Art. No. 214311.
(9) Clarkson, J. R.; Baquero, E.; Zwier, T. S. *J. Chem. Phys.* **2005**, *122* (21) Art. No. 214312.
(10) Dian, B. C.; Clarkson, J. R.; Zwier, T. S. *Science* **2004**, *303* (5661), 1169.
(11) Selby, T. M.; Zwier, T. S. *J. Phys. Chem. A* **2007**, *111* (19), 3710.
(12) van Mourik, T.; Emson, L. E. V. *Phys. Chem. Chem. Phys.* **2002**, *4* (23), 5863.
(13) Frisch, M. J. T., G. W.; Schlegel, H. B.; Scuseria, G. E.; Robb, M. A.; Cheeseman, J. R.; Montgomery, J. A., Jr.; Vreven, T.; Kudin, K. N.; Burant, J. C.; Millam, J. M.; Iyengar, S. S.; Tomasi, J.; Barone, V.; Mennucci, B.; Cossi, M.; Scalmani, G.; Rega, N.; Petersson, G. A.; Nakatsuji, H.; Hada, M.; Ehara, M.; Toyota, K.; Fukuda, R.; Hasegawa, J.; Ishida, M.; Nakajima, T.; Honda, Y.; Kitao, O.; Nakai, H.; Klene, M.; Li, X.; Knox, J. E.; Hratchian, H. P.; Cross, J. B.; Bakken, V.; Adamo, C.; Jaramillo, J.; Gomperts, R.; Stratmann, R. E.; Yazyev, O.; Austin, A. J.; Cammi, R.; Pomelli, C.; Ochterski, J. W.; Ayala, P. Y.; Morokuma, K.; Voth, G. A.; Salvador, P.; Dannenberg, J. J.; Zakrzewski, V. G.; Dapprich, S.; Daniels, A. D.; Strain, M. C.; Farkas, O.; Malick, D. K.; Rabuck, A. D.; Raghavachari, K.; Foresman, J. B.; Ortiz, J. V.; Cui, Q.; Baboul, A. G.; Clifford, S.; Cioslowski, J.; Stefanov, B. B.; Liu, G.; Liashenko, A.; Piskorz, P.; Komaromi, I.; Martin, R. L.; Fox, D. J.; Keith, T.; Al-Laham, M. A.; Peng, C. Y.; Nanayakkara, A.; Challacombe, M.; Gill, P. M. W.; Johnson, B.; Chen, W.; Wong, M. W.; Gonzalez, C.; Pople, J. A. *Gaussian 03*, revision C.02; Gaussian, Inc.: Wallingford, CT, 2004.
(14) Becke, A. D. *Phys. Rev. A* **1988**, *38* (6), 3098.
(15) Lee, C. T.; Yang, W. T.; Parr, R. G. *Phys. Rev. B* **1988**, *37* (2), 785.
(16) Frisch, M. J.; Pople, J. A.; Binkley, J. S. *J. Chem. Phys.* **1984**, *80* (7), 3265.
(17) Peng, C. Y.; Schlegel, H. B. *Isr. J. Chem.* **1993**, *33* (4), 449.
(18) Selby, T. M.; Meerts, W. L.; Zwier, T. S. *J. Phys. Chem. A* **2007**, *111* (19), 3697.
(19) Burgi, T.; Droz, T.; Leutwyler, S. *Chem. Phys. Lett.* **1995**, *246* (3), 291.
(20) Burgi, T.; Droz, T.; Leutwyler, S. *J. Chem. Phys.* **1995**, *103* (17), 7228.
(21) Kable, S. H.; Knight, A. E. W. *J. Chem. Phys.* **1990**, *93* (5), 3151.
(22) Schmitt, M.; Feng, K.; Boehm, M.; Kleinermanns, K. *J. Chem. Phys.* **2006**, *125* (14) Art. No. 144303.